Numerical analysis of a medium scale latent energy storage unit for districtheating systems

Cite this article as: Colella C, Sciacovelli A, Verda V. Numerical analysis of a medium scale latent energy storage unit for district heating systems, Energy 45 (2012) 397-406, doi: 10.1016/j.energy.2012.03.043

Numerical analysis of a medium scale latent energy storage unit for district heating systems

Francesco Colella[a*], Adriano Sciacovelli[a], Vittorio Verda[a]

[a] Politecnico di Torino, Dipartimento di Energetica, C.so Duca degli Abruzzi, 10129, Torino, Italy

Abstract:

The present paper describes the application of computational fluid-dynamics (CFD) to the design and characterization of a medium scale energy storage unit for district heating systems. The shell-and-tube LHTES unit contains a technical grade paraffin (RT100) and uses water as heat transfer fluid (HTF). The system has been designed to transfer heat from the primary to the secondary heat district heating networks. After an initial description of the LHTES unit and a wide literature overview on the subject, the paper discusses the need for thermal enhancement to improve the thermal conductivity of the phase change material (PCM). A solution based on a paraffin-graphite composite with a 15% graphite volume fraction has been found to be well performing in this particular application. Several operating scenarios characterized by heat requests ranging between 130kW and 400kW have been explored and the main outputs presented as function of *Re* and *St* numbers. The time-wise variations of other significant quantities such as liquid fraction, sensible and latent energy content, HFT outlet temperature and heat fluxes have been also presented and discussed. A final discussion on the possible system configurations shows that in comparison to traditional water storage systems for district heating, LHTES systems provide, depending on the chose alternative, higher energy storage densities.

Keywords:

Latent energy storage, phase change materials, district heating, CFD

* Corresponding author. Tel.: +39 011 5644478; Fax: +39 011564 4499; E-mail address: francesco.colella@polito.it

Cite this article as: Colella C, Sciacovelli A, Verda V. Numerical analysis of a medium scale latent energy storage unit for district heating systems, Energy 45 (2012) 397-406, doi: 10.1016/j.energy.2012.03.043

1. Introduction

District Heating is a rational way to provide heat to buildings located in a sufficiently dense urbanization. Indeed, heat may be produced by means of centralized plants which are more efficient than domestic boilers [1]. District heating systems are composed by one or more thermal plants, a distribution network of insulated pipes where hot water, superheated water or steam flow, delivering heat to the users. Fundamental elements of district heating networks are heat storage systems which are largely used to even the discrepancy between energy supply and demand. The storage system is charged during the night eventually by using CHP plants and discharged during the day when the thermal request peaks. This operation has significant energetic advantages, including a reduction in the primary energy consumption with respect to the separate production of heat and power, and also economic advantages related to a shift of a portion of electrical energy production to the daily hours [2].

Energy storing techniques can be classified in three main groups: sensible, latent and thermo-chemical heat storage. Latent heat thermal energy storage systems (LHTESS) are becoming increasingly attractive due to the low volume/energy ratio together with a small temperature change experienced during the charging and discharging processes. Indeed, latent heat energy storage systems are able of storing heat at a constant or almost constant temperature corresponding to the phase transition temperature of the Phase Change Material (PCM). Several comprehensive reviews on PCMs are available in the literature; the interested reader can refer to [3][4][5]. PCMs can be classified in two groups: organic and inorganic. Organic PCMs have several advantages including congruent melting, non-corrosive behaviour, compatibility with typical construction materials, chemically stability and low cost [6]. They can be further sub-divided in non-paraffin and paraffin organic the latter widely used as heat storage material due to the wide solidification temperature range and high latent heat. Inorganic PCMs show an almost two fold increase in the heat storage

Cite this article as: Colella C, Sciacovelli A, Verda V. Numerical analysis of a medium scale latent energy storage unit for district heating systems, Energy 45 (2012) 397-406, doi: 10.1016/j.energy.2012.03.043

capacity in comparison to organic PCMs and high thermal conductivity. Salt hydrates are typical inorganic compounds used as inorganic PCMs. Their main drawbacks include incongruent melting, poor nucleating properties and corrosive actions to many metals.

The main disadvantage of LHTESS is represented by the low thermal conductivity of the common phase change materials which drastically affects the performance of the units. This characteristic becomes evident during the energy charge and discharge processes that take place with considerable temperature drops and low melting/solidification rates. The application of PCMs in large scale units is still debated and is strongly dependent from the thermal performance enhancement of employed materials. Currently there are various techniques adopted for enhancing the thermal performance of LHTES units: use of extended surfaces (fins), use of multiple PCMs, enhancement of the thermal conductivity, PCM micro-encapsulation. A detailed review of the above mentioned techniques is out of the scope of this work, but the interested reader should refer to [7].

PCM units can be also classified on the basis of the PCM container configuration. The first class includes cylindrical units with the PCM filling the shell and the heat transfer fluid (HTF) flowing through a single inner tube. The second class includes cylindrical units with the HTF flowing in the shell and the PCM located in the single inner tube. The third group includes shell-and-tubes units commonly used to improve the heat transfer [8]. Several other applications use rectangular or spherical geometries. A comprehensive review on the issue is available in [5].

2. Literature overview

The literature on LHTES is particularly rich of contributions and therefore, for sake of simplicity, only the most significant works regarding cylindrical and shell-and-tube type applications will be reviewed. Experimental works on cylindrical and shell-and-tube type LHTES units have been performed by several authors. Choi and Kim studied the heat-transfer characteristics for circular finned and sing-tube units during the freezing of magnesium chloride hexahydrate (116.7°C melting temperature) [9]. A wide range of experimental setups have been considered by the authors

Cite this article as: Colella C, Sciacovelli A, Verda V. Numerical analysis of a medium scale latent energy storage unit for district heating systems, Energy 45 (2012) 397-406, doi: 10.1016/j.energy.2012.03.043

involving different HTF flow rates and inlet temperatures. Hasan [10] conducted an experimental investigation of a cylindrical storage system containing palmitic acid as PCM. The work presents detailed temperature measurements as well as other data regarding the solid-liquid interface propagation and the exchanged heat flux. Dimaano and Watanabe [11] conducted experimental observation on a thermal energy storage containing capric and lauric acids as PMCs. Sari and co-workers [12] performed some experimental observations on a LHTES systems containing and stearic acids as PCM. A similar analysis has been conducted by the same author on a cylindrical LHTES module containing eutectic mixtures of lauric and stearic acids and a mixture of mystiric and palmitic acids [13][14]. Most of the previous works investigate PCMs having low melting temperature, typically below 60 °C. A more recent experimental contribution from Agyenim and co-workers uses erythriol as PCM (117.7°C melting temperature) [15]. The authors investigated the thermal performance enhancement due to the addition of longitudinal and circular fins to a standard cylindrical LHTES unit. The performance of a shell-and-tube type LHTES in comparison to a single tube system has been analysed by the same authors in [16]. The results contained in the previous contributions show similar temperature profiles and solid-liquid interface progression during the charging and discharging processes.

A bulk part of the literature work is dedicated to the modelling of LHTES units. The literature survey conducted showed that the modelling of phase change materials is quite challenging due to complexity and the coupling of physical problems involved. In particular the heat transfer problem in the PCM is highly non linear due to the moving solid-liquid interface and analytical solutions are only known for moving boundary problems characterized by simple boundary conditions and geometries [6]. Further complexity is due to transient nature of phase change problems due to the solid-liquid interface movements. Therefore, the HTF temperature field would never reach a steady state regime. Furthermore for short pipes, due to the entrance effect, the flow would never develop fully developed conditions, making useless the adoption of empirical correlations for the evaluation of the heat transfer parameters. The literature review showed that solutions to phase change

Cite this article as: Colella C, Sciacovelli A, Verda V. Numerical analysis of a medium scale latent energy storage unit for district heating systems, Energy 45 (2012) 397-406, doi: 10.1016/j.energy.2012.03.043

problems are typically found by means of one-dimensional, two and three dimensional numerical models. A wide review on the different modelling technique is available in [17]. The energy equation implemented in the models is formulated mainly by using two methods: enthalpy method or temperature-based equivalent capacity methods, with the former being the most common approach. Enthalpy methods have the direct advantage that the PCM solid-liquid region is treated as a single domain, using a fixed grid without adopting explicit procedures for tracking the interface. The essence of this method is based on the inclusion of the latent heat term which appears in the energy equation as a source term which significantly simplifies the numerical treatment of the problem.

An enthalpy based formulation has been used by Lacroix [18] who developed a 2D numerical model to predict the transient behaviour of a shell-and-tube storage unit with n-octadecane as PCM. The heat transfer between PCM and HTF has been tackled by using empirical correlations for convective heat transfer problems. A constant heat transfer coefficient assumption has been also used by Ismail and Goncalves [19] which modelled and shell-and-pipe LHTES unit having *n*-eicosane (36.4°C melting temperature) and water as HTF. The assumption of constant heat transfer coefficient has been dropped by Cao and Faghri [20] who analysed the performance of a thermal storage module including the thermo-fluid-dynamics of the heat transfer fluid. A coupled thermo-fluid-dynamics analysis of shell-and-tube LHTES unit has been also presented by Ismail and Abugderah [21]. The work presents a wide range of numerical results including PCM temperature distributions, solid-liquid interface position and heat accumulated in the unit. A parametric analysis involving different system setups with variable HTF Reynolds number, Stefan number and melting temperature has been also presented. Anica [22] performed an experimental and numerical study of a LHTES unit which employs a technical grade paraffin as PCM. The author, also in this case, adopted an enthalpy formulation for the solution of the energy equation coupled with the thermo-fluid-dynamic model of HTF. The discharge process of a shell-and-tube LHTES unit containing KNO_3–$NaNO_3$ (220°C melting temperature) as PCM has been recently analyzed by Guo and Zhang

Cite this article as: Colella C, Sciacovelli A, Verda V. Numerical analysis of a medium scale latent energy storage unit for district heating systems, Energy 45 (2012) 397-406, doi: 10.1016/j.energy.2012.03.043

[23]. The enthalpy formulation has been adopted for the solution of the 2D heat transfer problem in the PCM volume, while the thermo-fluid-dynamics of the HTF has been ignored. A wall temperature boundary condition has been enforced instead. A parametric study has been conducted to assess how the performance of the storage system depends on the geometry of the unit and boundary conditions. The latest contribution considered in this literature survey has been developed by Adine and El Qarnia [24]. The authors conducted a 2D numerical analysis of the thermal behaviour of a shell-and-tube LHTES containing two PCMs: P116 (50°C melting temperature) and n-octadecane (27.7°C melting temperature). As in the previous contribution the paper presents and 2D heat transfer model of the PCM domain based on the enthalpy method while neglecting the thermo-fluid-dynamic behaviour of the HTF. Empirical correlations for the evaluation the convective heat transfer coefficient of the HTF have been used instead.

The present paper describes the application a finite volume CFD code FLUENT for the characterization of the discharge process in a medium scale shell-and-tube type LHTES unit. The heat transfer problem in the PCM domain solved using the classical enthalpy method, has been coupled to the thermo-fluid-dynamic problem of HTF. The unit is designed to cope with a maximum heat request around 400kW and is used to transfer heat from the primary district heating network working in the 120-65°C temperature range to the secondary user network which works in the 80-60°C temperature range. The charging and discharging process are therefore realized at two different temperature levels, 120°C and 80°C, respectively. The shell contains RT100 an organic paraffin characterized by a 99 °C melting temperature and medium heat of fusion 124 kJ/Kg [5]. The novelty of this work is represented by the characterization and design of a medium size and medium temperature LHTES unit, while all the literature works are dedicated to small-size solar applications. Indeed none of the experimental or numerical studies available in the literature refer to similar systems in terms of thermal request or melting temperature and usually are relative to small-scale lab devices. The total amounts of heat delivered to the HTF as well as the main output of the numerical analysis have been correlated in terms of the Stefan, and Reynolds numbers

Cite this article as: Colella C, Sciacovelli A, Verda V. Numerical analysis of a medium scale latent energy storage unit for district heating systems, Energy 45 (2012) 397-406, doi: 10.1016/j.energy.2012.03.043

3. Description of the unit

The LHTES unit consists of a metal shell and a 15×15 matrix of copper pipes (see figure 1). The heat transfer fluid, water in this work, is convected through the pipes exchanging heat with the PCM filling the shell space within the container and the tubes. The HTF tubes (12.5 mm i.d. and 1 mm thick), are 2.9 m long. A commercial grade paraffin RT100 has been used a PCM. Its thermo-physical properties, provided by the manufacturer, are resumed in Table 1.

The properties of the RT100 have been modified under the assumption that a high conductivity material (i.e. expanded natural graphite) is added to the PCM for improving its thermal conductivity. Indeed, according to Haillot and co-workers [26], the thermal conductivity of paraffin PCM could be increased by a factor of 10-300 depending on the density of the graphite matrix adopted. In this work, the conductivity enhancement factor has been chosen to be equal to 75 which corresponds to a graphite matrix density around 100 kg/m^3 and a volume fraction of natural expanded graphite φ in the composite around 15% [27].

The graphite-paraffin composite thermo-physical properties have been computed as described in [28] and presented hereafter

$$\rho_c = (1-\varphi)\rho_{PCM} + \varphi\rho_g \quad (1)$$

$$(\rho\, c_p)_c = (1-\varphi)(\rho\, c_p)_{PCM} + \varphi(\rho\, c_p)_g \quad (2)$$

$$(\rho\, L)_c = (1-\varphi)(\rho\, L)_{PCM} \quad (3)$$

where ρ is the density, c_p the specific heat, L the latent heat and the subscripts c, PCM and g refer to composite material, pure PCM and expanded natural graphite, respectively. The following thermo-physical properties of the pure graphite have been used: density equal to 2250 kg/m^3[27],

Cite this article as: Colella C, Sciacovelli A, Verda V. Numerical analysis of a medium scale latent energy storage unit for district heating systems, Energy 45 (2012) 397-406, doi: 10.1016/j.energy.2012.03.043

and specific heat equal to 709 J/kg/K [29]. The above referenced equations apply for the PCM both in the liquidus and solidus states.

The LHTES unit is used to store the heat delivered from the primary district heating (continuous lines in Figure 2) network which works in the 65-120°C temperature range. During the charging process, which takes place at night, the HTF delivers heat to the PCM which melts and stores the energy both in terms of sensible and latent forms. In this phase, valves P_{in} and P_{out} are open while valves S_{in} and S_{out} are closed. The discharging process, taking place during early morning hours with high thermal request, is characterized by the PCM solidification process. During this phase heat is transferred to the HTF circulating in the secondary user network which works in the 60-80°C temperature range. In this setup, valves P_{in} and P_{out} are closed while valves S_{in} and S_{out} are open. A schematic of the system is depicted in figure 2.

The numerical analysis of the PCM unit has been conducted for several different operative conditions. First, three main designs conditions are explored. In these scenarios the LHTES unit is operated in order to provide 100%, 50% and 25% of the maximum thermal request. In these conditions, the mass flow rate circulated through each of HTF pipes is equal to around 0.02 kg/s, 0.01 kg/s and 0.005 kg/s corresponding to *Re* equals to 2000, 1000 and 500, respectively. The discharge process is supposed to start with the liquid PCM in the unit at a temperature equal to 120°C corresponding to the maximum fluid temperature in the primary district heating network. Other operating scenarios characterized by inlet temperature ranging between 50°C and 70°C corresponding to *St* (Stefan number) in the 0.8-1.2 range, have been also explored.

4. Modelling

The fluid-dynamics behaviour of the HTF has been modelled using the classical Navier-Stokes equations arranged in axisymmetric fashion. The CFD analysis has been indeed limited to the domain region including one HTF pipe and the PCM portion associated with it. The boundaries of the computational domain considered in this study are depicted as dashed lines in figure 1.left and

Cite this article as: Colella C, Sciacovelli A, Verda V. Numerical analysis of a medium scale latent energy storage unit for district heating systems, Energy 45 (2012) 397-406, doi: 10.1016/j.energy.2012.03.043

1.right. The same approach has been considered by the vast majority of the numerical studies considered in the literature overview. For the region of the computational domain containing the PCM an enthalpy-porosity approach has been used since it does not require and explicit tracking of the solid-liquid interface [30]. The presence of the solid or liquid phase is instead monitored by using a quantity known as solid fraction. The *mushy zone* is the region where the liquid fraction lies between 0 and 1. The liquid fraction value controls also the fluid porosity which decreases from 1 to 0, being 0 for the solid phase where the velocities drop to zero [31].

The whole set of partial differential equations is resumed hereafter:

Continuity $$\frac{\partial \rho}{\partial t}+\frac{\partial \rho u_i}{\partial x_i}=0 \qquad (4)$$

Momentum $$\frac{\partial}{\partial t}\left(\rho u_i\right)+\frac{\partial}{\partial x_j}\left(\rho u_j u_i\right)=\mu\frac{\partial^2 u_i}{\partial x_j \partial x_j}-\frac{\partial p}{\partial x_i}+\rho g_i+S_i \qquad (5)$$

Energy $$\frac{\partial}{\partial t}\left(\rho \tilde{h}\right)+\frac{\partial}{\partial x_i}\left(\rho u_i \tilde{h}\right)=\frac{\partial}{\partial x_i}\left(k\frac{\partial T}{\partial x_i}\right) \qquad (6)$$

Where ρ is the fluid density, u the fluid velocity, x the spatial coordinate, t the time coordinate, μ the dynamic viscosity, p the pressure, S the momentum source term, $\tilde{h}$ the specific enthalpy and T the temperature. The specific enthalpy is defined as

$$\tilde{h}=h_{ref}+\int_{T_{ref}}^{T} c_p dt+\gamma L \qquad (7)$$

where h_{ref} is the enthalpy value at the reference temperature T_{ref} and γ is the liquid fraction. The latter is defined as

$$\gamma=0 \quad \text{if} \quad T<T_{solidus}$$

$$\gamma=1 \quad \text{if} \quad T>T_{liquidus}$$

$$\gamma=\frac{T-T_{solidus}}{T_{liquidus}-T_{solidus}} \quad \text{if} \quad T_{solidus}<T<T_{liquidus} \qquad (8)$$

Cite this article as: Colella C, Sciacovelli A, Verda V. Numerical analysis of a medium scale latent energy storage unit for district heating systems, Energy 45 (2012) 397-406, doi: 10.1016/j.energy.2012.03.043

The momentum source term in the enthalpy-porosity method is defined as

$$S_i = \frac{\left(1-\gamma^2\right)}{\left(\gamma^3+\varepsilon\right)} A_{mush} u_i \qquad (9)$$

where ε is a small number typically around 10^{-3} to avoid the division by zero and A_{mush} is the mushy zone constant which describe how steeply the velocity are reduced to zero when the material solidifies. The latter is usually a very large number, ranging between 10^4 to 10^8 kg/m^3/s. The effect of the mushy zone constant value has been investigated by Shmuely et al. [32]. They have found that this input parameter has an impact on the result and suggested a value around 10^8 kg/m^3/s. However, it must be stressed that Shmuely and co-workers have investigated the melting process while the current paper discusses the solification process where due to the negligible impact of the buoyancy the mushy zone constant has a minor effect. For this reason an average value equal to 10^6 kg/m^3/s has been chosen.

The HTF, PCM and wall material properties are supposed to be independent of the temperature. They may however be different, for the PCM, in the solid and liquid phases. The outer walls, represented as dashed lines in figure 1.left, can be accurately considered as adiabatic. A velocity boundary condition has been enforced at the HTF inlet, where also the temperature is assumed to be known. A pressure outlet boundary condition has been enforced at the HTF outlet surface. The natural convection in the liquid phase of the PCM has been ignored. This assumption has been validated by several literature contributions [7][35]. These confirmed that during the discharge process of LHTES systems and the consequent solidification of the PCM, the heat transfer is dominated by conduction while natural convection exists only at the beginning of the process. The effect of natural convection is also minimized due to the vertical arrangement of the unit as has been also observed in [12].

The modelling has been conducted by using the finite-volume CFD code, FLUENT. In this particular application a segregated solver has been used to address the Navier–Stokes problem. The

Cite this article as: Colella C, Sciacovelli A, Verda V. Numerical analysis of a medium scale latent energy storage unit for district heating systems, Energy 45 (2012) 397-406, doi: 10.1016/j.energy.2012.03.043

fluid has been considered incompressible and the SIMPLE algorithm has been adopted to solve the pressure-velocity coupling.

The convective fluxes and have been approximated by using a second-order upwind scheme. Temporal discretization has been treated by using a second order implicit time integration scheme which has the advantage of being unconditionally stable with respect to the time step size. The effect of the time step size and integration scheme has been also assessed. Several simulations characterized by different time step sizes and higher order integration schemes have been conducted in order to assess whether or not time-step independent solutions were reached. Due to the neglected buoyancy effects during the solidification process, time step-independent solutions have been found using a time-step size ranging between 0.1 and 0.5 s.

A structured meshing approach has been used. Once produced a base mesh case, the grid has been systematically refined in order to assess whether or not a grid-independent solution was reached. The refining has been iterated until no substantial variations both in the local field data and integral values were observed. The mesh adopted for the simulations contains around 100k-cells. A schematic of the inlet region is presented in figure 3.

An iterative time-advancement scheme has been used where all the equations, for a given time-step, are solved iteratively in a segregated fashion, until the convergence criteria are met. The under-relaxation factors for the velocity components, pressure correction, density, energy and liquid fraction are equal to 0.7, 0.3, 1, 1 and 0.9.

The simulations have been considered to be converged when the scaled residuals were lower than 10^{-6} with the exception of the energy equation where the maximum allowed value was 10^{-8}. The degree of convergence of the solution has been estimated also by monitoring integral values of relevant quantities during the solution procedure.

The developed model has been validated by the authors against experimental results for shell-and-tube LHTES units. In particular references [33] and [34] present wide validation studies that confirm the ability of the model in predicting the behaviour of this kind of systems. Indeed both the

Cite this article as: Colella C, Sciacovelli A, Verda V. Numerical analysis of a medium scale latent energy storage unit for district heating systems, Energy 45 (2012) 397-406, doi: 10.1016/j.energy.2012.03.043

manuscripts pointed out that the developed model was able of providing good quantitative agreement between the simulations and experimental data both for charge and discharge processes.

5. Numerical results

The thermo-fluid-dynamics behaviour of the LHTES unit is presented in this section. A large set of numerical experiments have been conducted in order to analyze the transient heat transfer during the solidification process of the PCM. For sake of simplicity a detailed analysis of the CFD results will be presented for the design case characterized by a mass flow rate of HTF around 0.02 kg/s, *Re* equal to 2000 and *St* equal to 1. The global behaviour of the unit under different operating conditions, (i.e. different *Re* and *St* numbers) will be also presented towards the end of this section.

Figure 4 presents the velocity contours in the HTF pipe as computed by the CFD tools for the design case. The velocity profile representation shows that fully developed flow conditions are established at a distance from the inlet around 1.25 m. This finding confirms as already pointed out in [20] and [22], that the adoption of empirical correlations for heat transfer in fully developed flow conditions may result in a significant error for the evaluation of the system performance, especially for short LHETS units.

Figure 5 presents the temperature contours inside PCM and the HTF for the design case. The plot shows how the temperature profiles inside the PCM and consequently in the HTF domain do not reach steady state conditions due to the moving solidification front. The use of empirical correlations for characterizing the heat transfer to the HTF should be avoided also for this reason. The time dependent evolution of the solidification front inside the PCM domain has been plotted in figure 6 as function of the time.

It can be seen that the solidification process starts at the exterior side of the HTF pipe walls and propagate towards the outlet following the same temporal evolution of the temperature profile. The front propagates in the radial as well as in the axial directions showing significantly larger axial

Cite this article as: Colella C, Sciacovelli A, Verda V. Numerical analysis of a medium scale latent energy storage unit for district heating systems, Energy 45 (2012) 397-406, doi: 10.1016/j.energy.2012.03.043

velocities. Indeed, it reaches the external surface of the PMC domain after 1000 s, when, in the vicinity of the HFT pipe walls at the same moment, it has travelled for more than 2 m. This phenomena has been observed by several authors including [18][20][21][22]. The complete solidification of the PCM is reached after ca. 5000s from the starting of the discharge process.

The effect of the HTF Reynolds number on the total PCM liquid fraction has been plotted in figure 7.left. The analysis has been conducted for a constant *St* number and three different *Re* numbers, nominally, 2000, 1000 and 500. As typical for any system involving forced convection, the effect of *Re* on the evolution of the system liquid fraction is large. The solidification time indeed shows a one fold increase when *Re* is reduced from 2000 to 500 as depicted in figure 7.right. A similar result has been also found by Kuravi and co-workers [36]. As obvious the same large impact has been found when correlating HTF Reynolds number and position of the solidification front.

Figure 8 present the effect of *St* number on the temporal evolution of the liquid fraction in the unit and the solidification time. The parametrical study has been conducted keeping the HTF *Re* number equal to 2000 while the *St* number has be varied ranging between 0.8 and 1.2 corresponding to HTF inlet temperatures ranging between 50°C and 70°C. The reason for keeping such a limited *St* number range is given by the particular application the unit has been designed for. It must indeed operate in the temperature interval between 120°C and 80°C and transfer heat from the primary to the secondary district heating network. Figure 8.left shows how larger *St* numbers lead to shorter solification time indicating a better thermal performance of the unit. This phenomenon is due to the increase in the temperature difference between the HTF ad the PCM temperature. The increase in the solidification time as function of the *St* number is plotted in figure 8.right. The plot shows how a 35% reduction of the *St* number induces a 70% increase in the PCM solidification time.

The time wise variation of the sensible, latent and total energy stored is presented in figure 9. During the early stages of the discharge process (t<2000s) the energy delivered to the HTF comes mainly from the sensible part as confirmed by the higher slope of the sensible heat curves depicted in figure 9.left. This stage is then followed by a second stage during which the sensible energy

Cite this article as: Colella C, Sciacovelli A, Verda V. Numerical analysis of a medium scale latent energy storage unit for district heating systems, Energy 45 (2012) 397-406, doi: 10.1016/j.energy.2012.03.043

content of the PCM remains almost constant, and most of the energy released comes from the latent part. The duration of this phase depends significantly on the HTF *Re* number being larger for lower *Re.* The discharge process then proceeds towards the last stage characterized by an almost equal sensible and latent energy release. This last stage is characterized by the sensible and latent heat curves having a comparable slope (see figure 9) and typically starts when the percentage of PCM in the solid phase ranges between 75% and 80%. The same stages have been identified by Adine and El Qarnia [24] who investigated the charging process of a LHTES unit containing paraffin as PCM. The effects of variable *Re* and *St* numbers on the time wise variation of the PCM total energy content are presented in figure 9.centre and 9.left, respectively. An almost linear behaviour can be observed in both the figures confirming that the discharge process proceeds with an almost constant heat transfer rate which tends to lower during the last stage of the process. Same behaviour has been observed by [20] and [24]. Both the figures also confirm that a more effective heat transfer can be achieved when running the system with larger *Re* and *St* numbers.

The effects of *Re* and *St* number variation on the temporal evolution of the heat flux per unit area are presented in figure 10.left and 10.right, respectively. As previously described, larger heat fluxes can be achieved by increasing the HTF *Re* and *St* numbers. Figure 10.left shows that the lower is the HTF *Re* number the more constant is heat transfer rate during the process. The latter shows indeed a steeper decrease during the first stage when the discharge of the unit takes place with larger *Re*. Figure 10.left shows how the *St* number does not affect the shape of the heat flux profile. A uniform up-ward translation of the heat flux profiles is achieved for larger *St* numbers, instead. It is worth to note how the heat flux profiles represented in both figures 10.left and 10.right reflect the 3 stage behaviour of the discharge process.

Another significant variable affecting the performance of the LHTES unit is the HTF outlet temperature. This must be somehow higher than a minimum threshold in order to assure proper operating conditions for the secondary heating network. The analysis conducted hereafter is based on the assumption that the minimum allowable outlet temperature is 2 °C below the design value,

Cite this article as: Colella C, Sciacovelli A, Verda V. Numerical analysis of a medium scale latent energy storage unit for district heating systems, Energy 45 (2012) 397-406, doi: 10.1016/j.energy.2012.03.043

being the latter 80°C. Figure 11 shows the time wise evolution of the HTF outlet temperature and its dependence on the *Re* number. The outlet temperature threshold is represented as a horizontal dashed line in the plot. It can be clearly seen that the larger the *Re* the shorter is the LHTES unit available time, being the latter equal to 1700 s, 6100 s and 10400 s for *Re* equal to 2000, 1000 and 500, respectively.

During such time intervals the average heat flux that each pipes of the unit delivers to the HTF is equal to 1.77 kW, 0.95 kW and 0.58 kW for *Re* equals to 2000, 1000 and 500, respectively. The global unit, comprehensive of the 225 HTF pipes, is therefore able of supplying the secondary network with a 400kW, 220kW and 130kW heat flux for 1700 s, 6100 s and 10400 s respectively. The overall energy amount supplied to the users is equal to 675 MJ, 1330 MJ and 1340 MJ being larger for operating regimes characterized by lower *Re* numbers. This phenomenon is due to the lower outlet temperatures observed when *Re* is equal to 2000 that causes only the 42% of the total energy, sensible and latent, to be used (see figure 9.centre). This percentage increases up to 95.5% and 99.9% for *Re* equal to 1000 and 500, respectively. Operative conditions characterized by lower *Re* numbers are therefore desirable, with higher thermal requests covered by LHETS units having a larger number of HTF pipes, rather than higher mass flow rates in each single pipe. The previous conclusions are supported by the temperature and liquid fraction contours in the LHTES unit for the three operating regimes (*Re* equal to 2000, 1000 and 500) at 1700 s, 6100 s and 10400 s (see figure 12). It can be clearly see that at the moment when the outlet temperature drops below the lower limit, the system operating with *Re* equal to 500 experiences much lower temperature and liquid fraction in comparison to the others confirming a better sensible and latent energy utilization.

6. System configuration and comparison to alternatives

This section analyses the possible configurations of a district heating system in presence of traditional water-based and LHTES units. The system layout considered in this work has been defined in order to charge of the LHTES unit using the primary district heating network in the 120-

Cite this article as: Colella C, Sciacovelli A, Verda V. Numerical analysis of a medium scale latent energy storage unit for district heating systems, Energy 45 (2012) 397-406, doi: 10.1016/j.energy.2012.03.043

65°C temperature range and to discharge it using the building heating network in the 60-80°C temperature range. The resulting system layout is presented in Figure 12. It consists of the LHTES unit and a traditional district heating heat exchanger connected in parallel. The LHTES unit is also equipped with a bypass system designed in order to control flow through the storage system and consequently the temperature of the water returning to the building user network. Eventually, if the thermal request of the building is higher or the LHTES unit has been completely discharged, the traditional heat exchanger can be used to fulfil the energy request.

Besides the above mentioned solution (indicated hereafter as configuration 1), 4 other different alternatives including traditional and latent heat storage systems can be taken into account:

2. Traditional water storage system on the primary district heating network (120-65°C).
3. LHTES unit on the primary district heating network (120-65°C).
4. Traditional water storage system on the building heating network (80-60°C).
5. LHTES unit on the building heating network (80-60°C).

The performance of all the previous energy storage alternatives has been investigated in terms of theoretical energy storage density. The results are presented in Figure 13 in terms of temperature difference and energy storage density. The plots have been traced considering the specific heat capacity of the PCMs and the latent heat. The curve relative to the water based energy storage system has been build considering a constant heat capacity for the water. Depending on the working temperatures of the specific configuration different phase change materials have been chosen namely RT100 (solidification temperature around 99°C) and stearic acid (solidification temperature around 68°C). The corresponding working points are also identified on the plot.

The comparison between configuration 2 and 3 (water and latent energy storage on the primary district heating network) shows that no significant improvements in terms of energy storage density can be obtained using phase change materials due to the high operative temperature difference. On the contrary a conspicuous increase in the energy storage density in favour of LHTES systems is

Cite this article as: Colella C, Sciacovelli A, Verda V. Numerical analysis of a medium scale latent energy storage unit for district heating systems, Energy 45 (2012) 397-406, doi: 10.1016/j.energy.2012.03.043

observed comparing configuration 4 and 5 (energy storage on the building heating network). In general it must be pointed out that configuration 1 and 5 (latent heat storage located on the building heating network) have the advantage of being decentralized, and providing high storage densities at ambient pressure and high energy efficiency. Indeed the losses due to thermal stratification typically encountered in traditional water energy storage systems are avoided in LHTES units [37]. However, in both the previous configurations when due to specific operating conditions the simultaneous use of the heat exchanger and the storage unit is required, higher water temperature on the return of the primary district heating network can be expected. This phenomenon which is marginal if only a limited number of latent energy storage systems are installed, becomes significant in presence of a large number of LHTES units.

Configuration 3 has the disadvantage of needing additional auxiliary boilers that are required to increase the temperature of the water leaving the storage system to its nominal value (120°C). Indeed, since the maximum charging temperature of the LHTES unit is equal to 120°C, the maximum temperature of the water leaving the unit (during the discharging process) will be below the 120°C threshold and additional heaters are constantly required.

7. Conclusions

The discharging behaviour of a medium scale LHTES unit has been characterized by means of CFD. The unit contains a 15×15 matrix of vertical HTF pipes immersed in a technical grade paraffin used as PCM. The storage unit is charged during the night eventually by using CHP plants and discharged during the day when the thermal request peaks. The paper discusses the needs for improving the thermal conductivity of the PCM in order to achieve the heat fluxes required for medium scale applications. A natural expanded graphite matrix has been found to guarantee the required conductivity enhancement without significantly compromising the other thermo-physical properties of the PCM. The behaviour of the unit has been studied in several different discharging scenarios characterized by variable *Re* and *St* numbers. Several outputs including time wise

Cite this article as: Colella C, Sciacovelli A, Verda V. Numerical analysis of a medium scale latent energy storage unit for district heating systems, Energy 45 (2012) 397-406, doi: 10.1016/j.energy.2012.03.043

variation of liquid fraction, PCM temperatures, sensible and latent energy, HTF outlet temperature have been presented. The unit has been shown to be able of covering a 130 kW to 400 kW heat request depending on the operating conditions.

The paper presents also a discussion on all the possible configurations of a district heating system based on traditional water-based and LHTES units. The analysis shows that the most performing options in terms of energy storage density are characterized by latent storage units installed on the building heating network rather than on the primary district heating network.

References

[1] Lund H., Möller B., Mathiesen B.V., Dyrelund A. The role of district heating in future renewable energy systems. Energy 2010; 35: 1381-1390.

[2] Fruergaard T., Christensen T.H., Astrup T. Energy recovery from waste incineration: Assessing the importance of district heating networks. Waste Management 2009; 30: 1264-1272.

[3] Zalba, B., Marin, J.M., Cabeza, L.F., Mehling, H. Review on thermal energy storage with phase change: materials, heat transfer analysis and applications. Appl. Therm. Eng 2003; 23, 251–283.

[4] Farid, M.M., Khudhair, A.M., Razack, S.A.K., Al-Hallaj, S. A review on phase change energy storage: Materials and applications. Energy Convers. Manage. 2004; 45, 1597– 1615.

[5] Agyenim, F., Hewintt, N., Eames, P., Smyth, M. A review of materials, heat transfer and phase change problem formulation for latent heat thermal energy storage systems (LHTESS), Renewable and sustainable Energy Reviews 2010; 14: 615-628

[6] Anica T. An experimental and numerical investigation of heat transfer during technical grade paraffin melting and solidification in a shell-and-tube latent thermal energy storage unit. Solar energy 2005; 79: 648-660.

Cite this article as: Colella C, Sciacovelli A, Verda V. Numerical analysis of a medium scale latent energy storage unit for district heating systems, Energy 45 (2012) 397-406, doi: 10.1016/j.energy.2012.03.043

[7] Jegadheeswaran, S., Sanjay, D. P. Performance enhancement in latent heat thermal storage system: a review. Renewable and Sustainable Energy Reviews 2009; 13: 2225-2244.

[8] Agyenim, F., Eames, P., Smyth, M. Heat transfer enhancement in medium temperature thermal energy storage system using a multitube heat transfer array. Renewable Energy 2010; 35: 198–207

[9] Choi,. J.C., Kim, S.D. Heat-transfer characteristics of a latent heat storage system using $MgCl{\cdot}6H_2O$, Energy 1992; 17(12): 1153-1164,

[10] Hasan, A. Phase change material energy storage system employing palmitic acid. Sol. Energy, 1994; 52, 143–154.

[11] Dimaano, M.N.R., Watanabe, T., Performance investigation of the capric and lauric acid mixture as latent heat energy storage for a cooling system. Sol. Energy, 2001; 72, 205– 215.

[12] Sari, A., Kaygusuz, K. Thermal energy storage system using stearic acid as a phase change material. Sol. Energy, 2001; 71, 365–376.

[13] Sari, A., Kaygusuz, K. Thermal performance of a eutectic mixture of lauric and stearic acids as pcm encapsulated in the annulus of two concentric pipes. Sol. Energy 2002; 72, 493–504.

[14] Sari, A., Thermal characteristics of a eutectic mixture of myristic and palmitic acids as phase change material for heating applications. Appl. Therm. Eng. 2003; 23, 1005–1017.

[15] Agyenim, F., Eames, P., Smyth, M. A comparison of heat transfer enhancement in a medium temperature thermal energy storage heat exchanger using fins. Solar Energy. 2009 83, 1509–1520.

[16] Agyenim, F., Eames, P., Smyth, M. Heat transfer enhancement in medium temperature thermal energy storage system using a multitube heat transfer array. Renewable Energy. 2010. 35, 198–207

Cite this article as: Colella C, Sciacovelli A, Verda V. Numerical analysis of a medium scale latent energy storage unit for district heating systems, Energy 45 (2012) 397-406, doi: 10.1016/j.energy.2012.03.043

[17] Verma P., Varun, Singal, S.K. Review of mathematical modeling on latent heat thermal energy storage systems using phase-change material. Renewable and Sustainable Energy Reviews, 2008, 12: 999−1031

[18] Lacroix, L. Numerical simulation of a shell-and-tube latent heat thermal energy storage unit. Solar energy, 1993, 50(4): 357-367

[19] Ismail, K.A.R., Goncalves, M.M. Thermal performance of a pcm storage unit. Energy Conversion & Management, 1999; 40: 115-138

[20] Cao, Y., Faghri A. Performance characteristics of a thermal energy storage module: a transient PCM/forced convection conjugate analysis. Int. J. Heat Mass Transfer, 1991; 34: 93-101

[21] Ismail, K. Abugderah, M. Performance of a thermal storage system of the vertical tube type. Energy Conversion & Management, 2000; 41: 1165-1190

[22] Anica Trp. An experimental and numerical investigation of heat transfer during technical grade paraffin melting and solidification in a shell-and-tube latent thermal energy storage unit. Solar Energy 2005; 79:648–660

[23] Guo, C., Zhang, W. Numerical simulation and parametric study on new type of high temperature latent heat thermal energy storage system. Energy Conversion and Management, 2008, 49: 919–927

[24] Adine H., A., El Qarnia, H. Numerical analysis of the thermal behaviour of a shell-and-tube heat storage unit using phase change materials. Applied mathematical modelling, 2009, 33: 2132-2144

[25] Rubitherm Technologies GmbH. Phase Change Material based on n-Paraffins and Waxes. – Available at: <http:// www.rubitherm.com/> [accessed 26.2.2011].

[26] Haillot D, Py X, Goetz V, Benabdelkarim M. Storage composites for the optimization of solar water heating systems. Chem Eng Res Design 2008; 86:612–7.

Cite this article as: Colella C, Sciacovelli A, Verda V. Numerical analysis of a medium scale latent energy storage unit for district heating systems, Energy 45 (2012) 397-406, doi: 10.1016/j.energy.2012.03.043

[27] Py, X., Olives, R., Mauran, S., Paraffin/porous-graphite-matrix composite as high and constant power thermal storage material. International journal of heat and mass transfer 2001, 44:2727-2737

[28] Kohodadadi, J. M., Hosseinizadeh, S.F., Nanoparticle-enhanced phase change materials (NEFCM) with great potential for improved thermal energy storage. International communications in heat and mass transfer, 2007; 34: 534-543

[29] Incropera, F.P., De Witt, D., Bergman, T.L., Lavine, A.S., Fundamentals of heat and mass transfer, sixth edition, Wiley & Sons Ltd; 2007.

[30] A.D. Brent, V.R. Voller, K.J. Reid, Enthalpy-porosity technique for modeling convection–diffusion phase change: application to the melting of a pure metal, Numer. Heat Transfer, 1988; 13: 297–318.

[31] Fluent Inc. FLUENT 6.2 user's guide; 2005.

[32] Shmueli, H., Ziskind, G., Letan, R., Melting in a vertical cylindrical tube: numerical investigation and comparison with experiments, International Journal of Heat and Mass Transfer 2010; 53: 4082-4091.

[33] Sciacovelli A., Verda V., Colella F. Numerical Model for Storage Systems Based on Phase Change Materials. Proceedings of IMECE '11: 2011 ASME International Mechanical Engineering Congress & Exposition. November 11 - 17, 2011, Denver, Colorado.

[34] Sciacovelli A., Verda V. Numerical analysis on melting in a cylindrical heat storage capsule. THERMACOMP 2011, Second International Conference on Computational Methods for Thermal Problems. September 5 – 7, 2011 Dalian, China.

[35] Lamberg P. Approximate analytical model for two-phase solidification problem in a finned phase-change material storage. Appl Energy 2004;77: 131–52.

[36] Kuravi, S., Trahan, J., Rahman, M.M., Goswami, D., Y., Stefanokos, E.K., Analysis of the transient heat transfer in a thermal energy storage module, Proceedings of the ASME 2010

International Mechanical Engineering Congress & Exposition, IMECE2010 November 12-18, 2010, Vancouver, Canada.

[37] Verda V. Colella F. Primary Energy savings through thermal storage in district heating networks, Energy (2011), 36(7): 4278-4286, doi:10.1016/j.energy.2011.04.015

Cite this article as: Colella C, Sciacovelli A, Verda V. Numerical analysis of a medium scale latent energy storage unit for district heating systems, Energy 45 (2012) 397-406, doi: 10.1016/j.energy.2012.03.043

Figure list

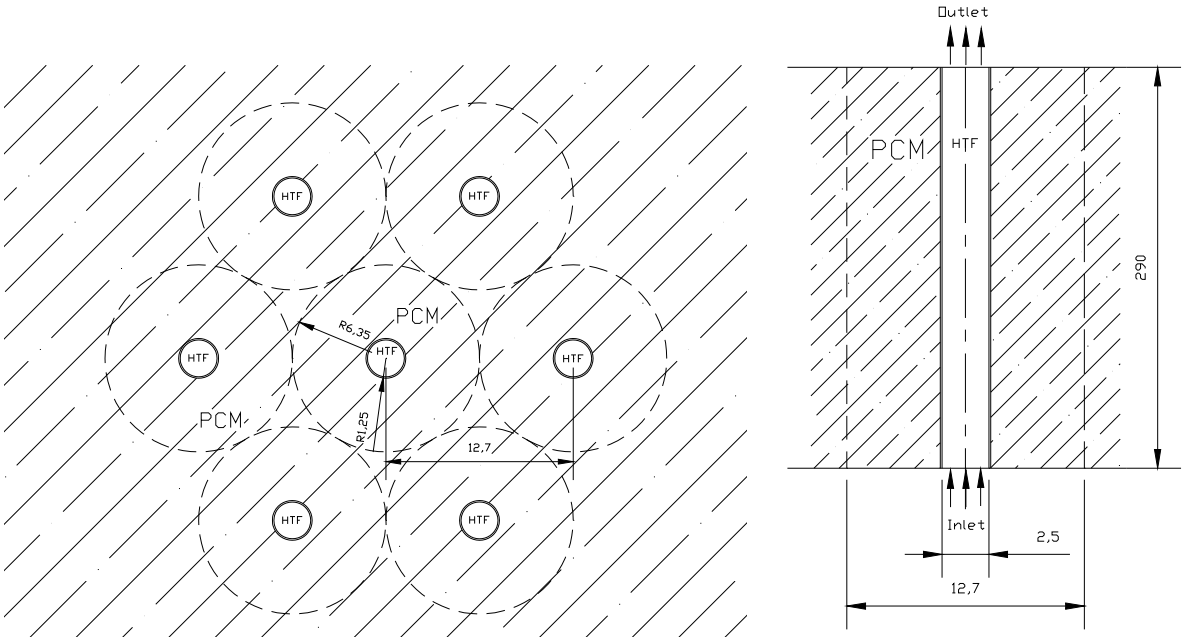

Fig. 1. LHTES unit schematic. Left) Unit Cross-section. Right) Single HFT longitudinal section (not to scale). Dimensions are expressed in cm.

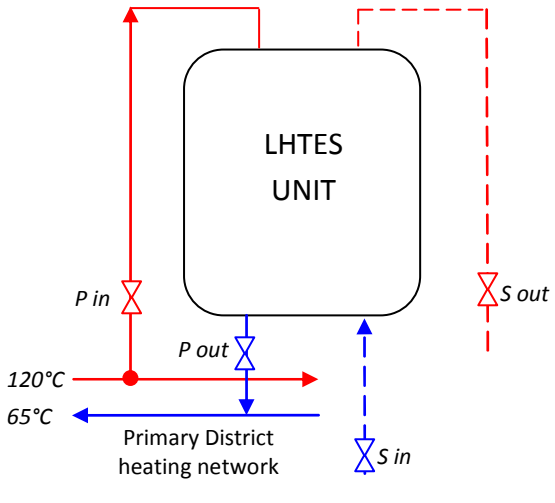

Fig. 2. Schematic of the connections between LHTES unit, primary and secondary district heating networks

Cite this article as: Colella C, Sciacovelli A, Verda V. Numerical analysis of a medium scale latent energy storage unit for district heating systems, Energy 45 (2012) 397-406, doi: 10.1016/j.energy.2012.03.043

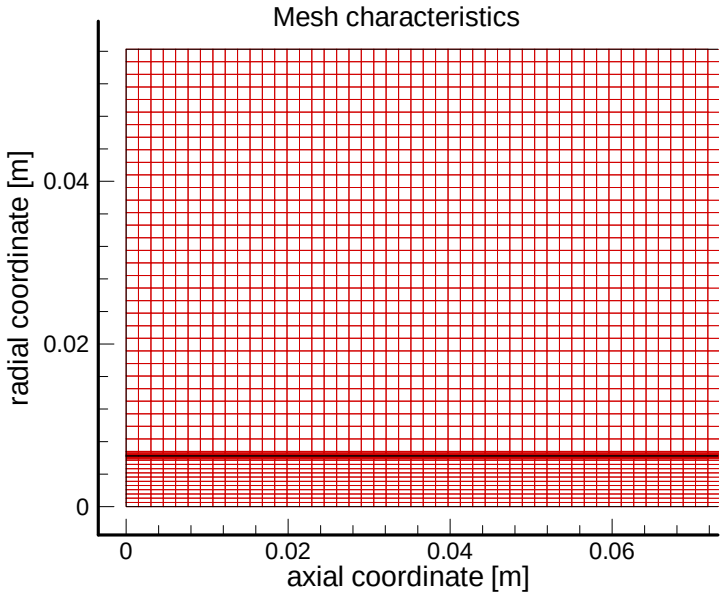

Fig. 3. LHTES meshing pattern

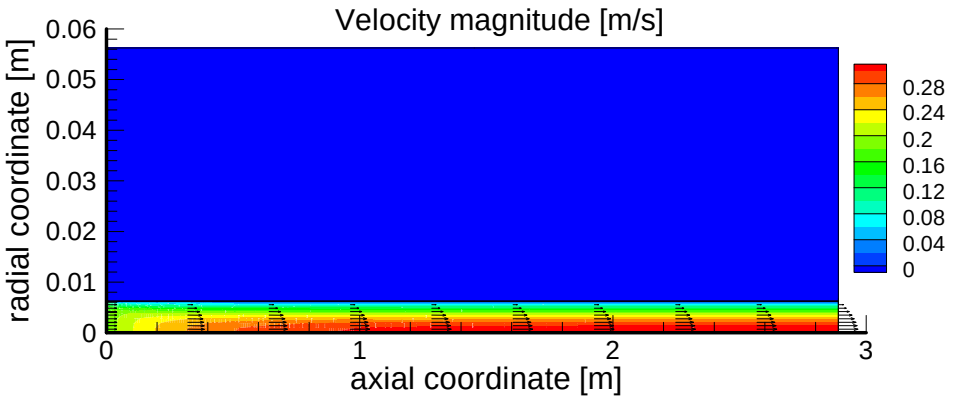

Fig. 4. Velocity contours in the HTF pipe for the design case. HTF mass flow rate 0.02 kg/s; Re=2000; St=1. (Not to scale)

Cite this article as: Colella C, Sciacovelli A, Verda V. Numerical analysis of a medium scale latent energy storage unit for district heating systems, Energy 45 (2012) 397-406, doi: 10.1016/j.energy.2012.03.043

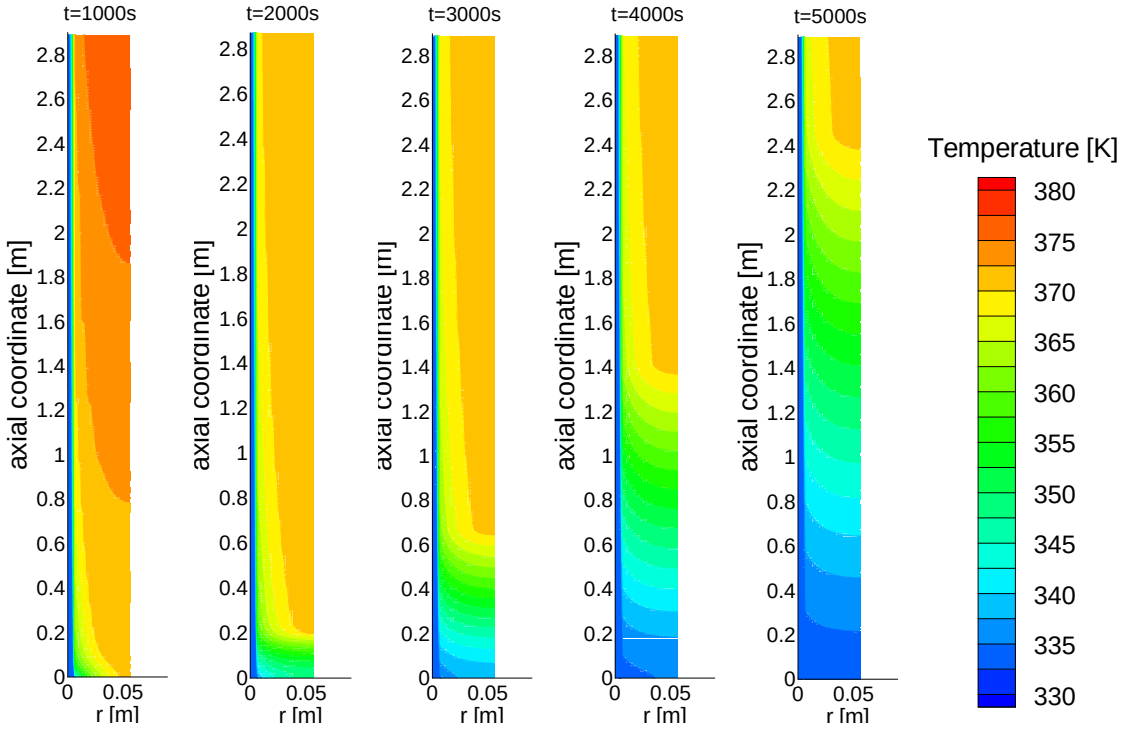

Fig. 5. Temperature contours in the HTF and the PCM region for the design case. HTF mass flow rate 0.02 kg/s; Re=2000; St=1. (Not to scale)

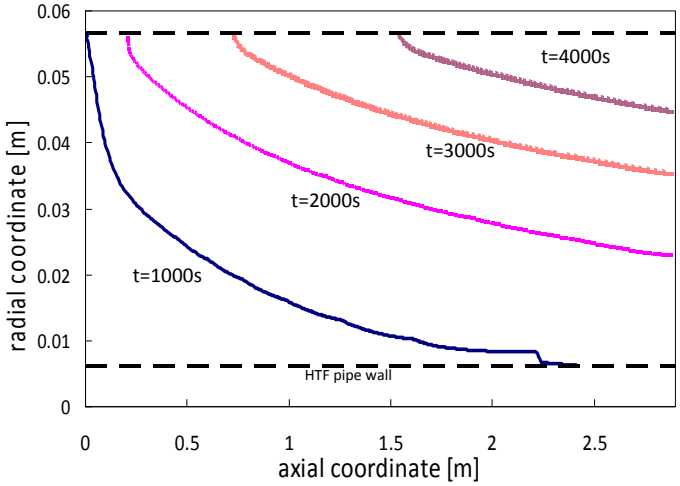

Fig. 6. Temporal evolution of the solification front for the design case. HTF mass flow rate 0.02 kg/s; Re=2000; St=1.

Cite this article as: Colella C, Sciacovelli A, Verda V. Numerical analysis of a medium scale latent energy storage unit for district heating systems, Energy 45 (2012) 397-406, doi: 10.1016/j.energy.2012.03.043

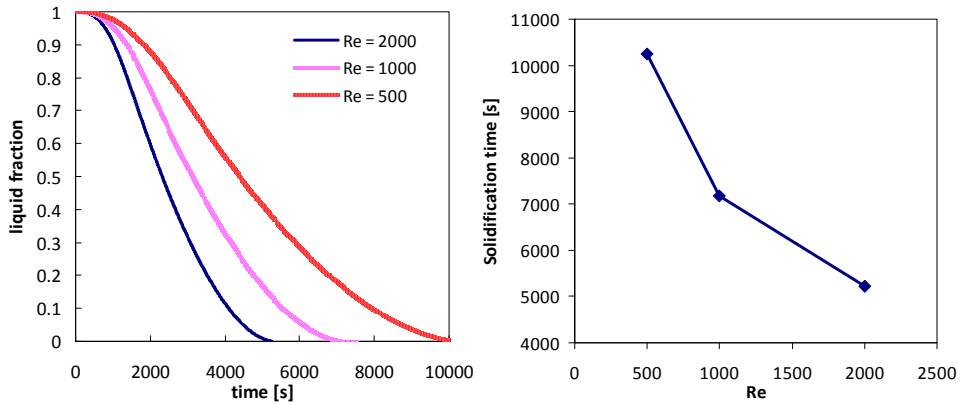

Fig. 7. left) Effect of the HTF Re number on the temporal evolution of the liquid fraction. HTF mass flow rate 0.02 kg/s (Re=2000), 0.01 kg/s (Re=1000), 0.005 kg/s (Re=500); St=1. Right) Effect of Re on the solidification time.

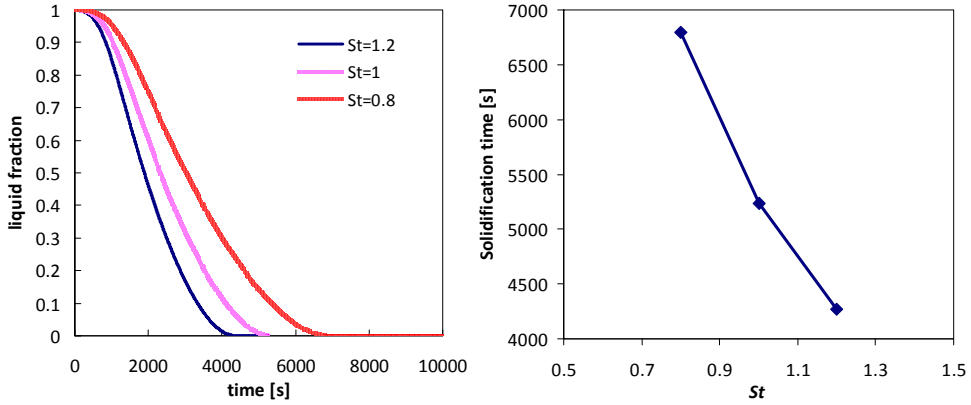

Fig. 8. left) Effect of the Stefan Number on the temporal evolution of the liquid fraction. HTF inlet temperature 50°C (St=1.2), 60°C (St=1.0), 70°C (St=0.8); Re=2000. Right) Effect of St on the solidification time.

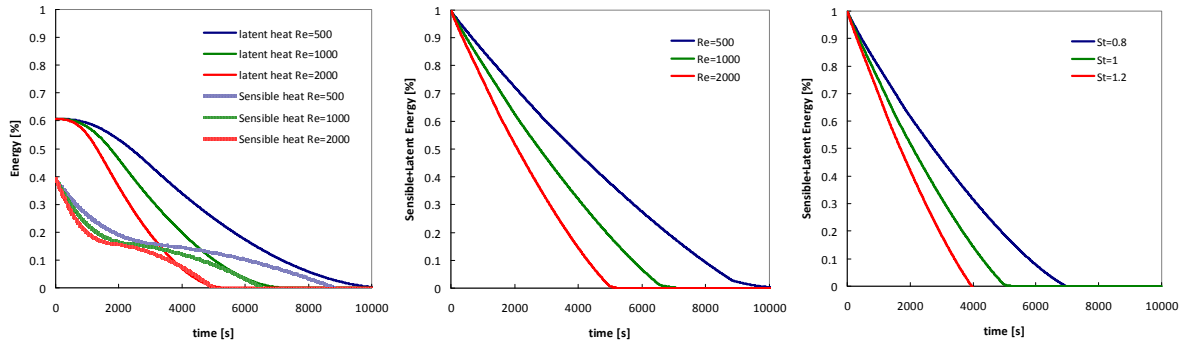

Fig. 9. left) Effect of Re number on the timewise variations of sensible and latent energy. centre) timewise vatiations of the total energy for different Re numbers. Right) timewise variation of total energy for different St numbers.

Cite this article as: Colella C, Sciacovelli A, Verda V. Numerical analysis of a medium scale latent energy storage unit for district heating systems, Energy 45 (2012) 397-406, doi: 10.1016/j.energy.2012.03.043

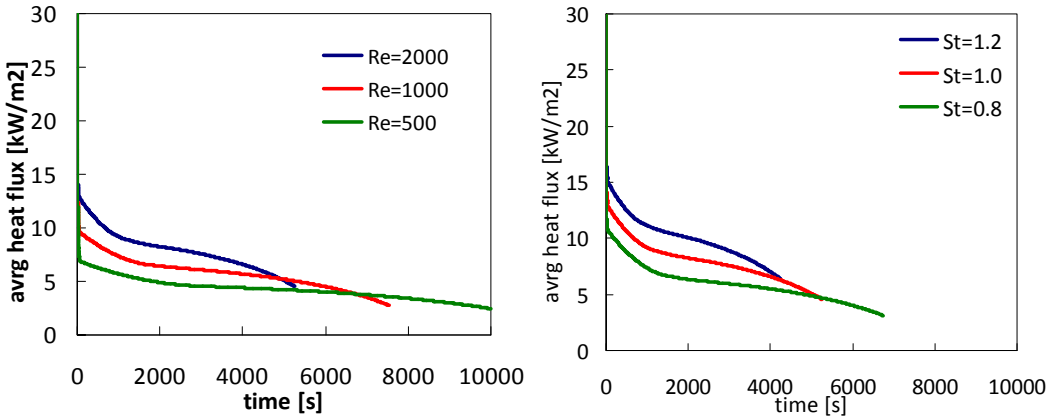

Fig. 10. left) Effect of Re number on the timewise variations of average heat flux per unit area. right) Effect of St number on the timewise variations of average heat flux per unit area.

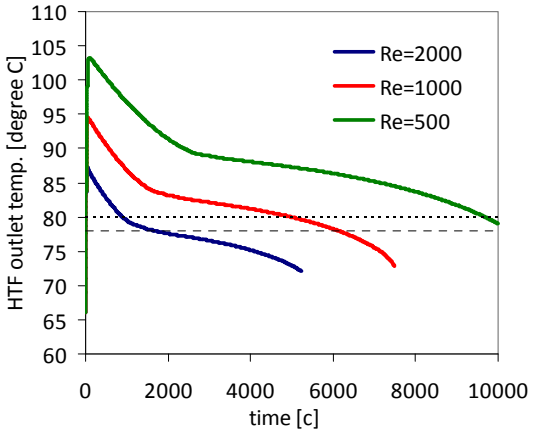

Fig. 11. Effect of Re number on the timewise variations of the HTF outlet temperature.

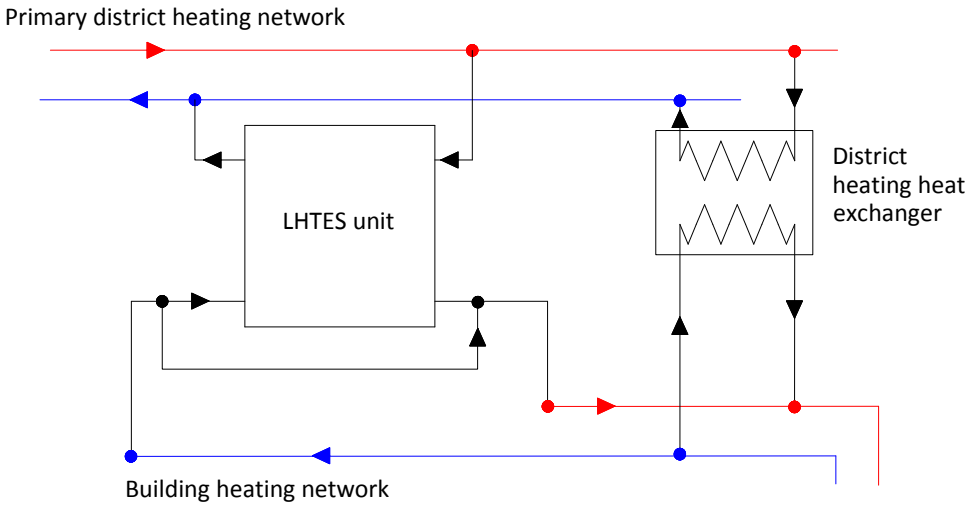

Fig. 12. System layout for configuration 1

Cite this article as: Colella C, Sciacovelli A, Verda V. Numerical analysis of a medium scale latent energy storage unit for district heating systems, Energy 45 (2012) 397-406, doi: 10.1016/j.energy.2012.03.043

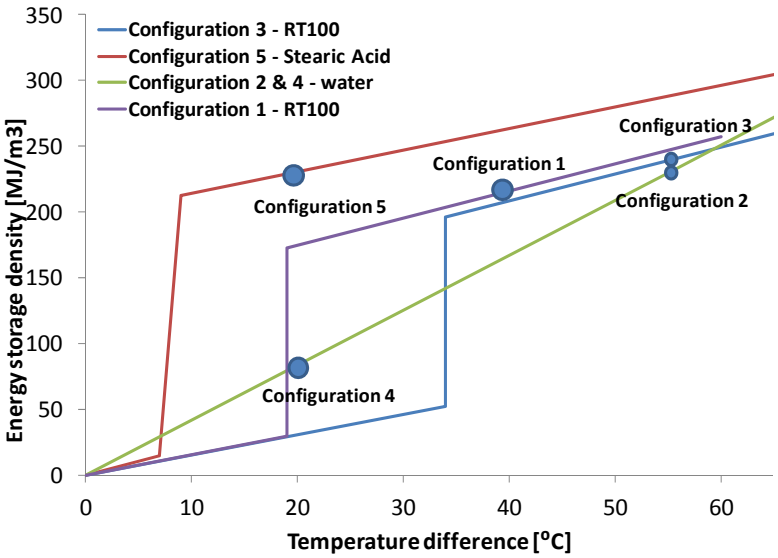

Fig. 13. Comparison of the different system configurations in terms of temperature difference and energy storage density.

Table list

Table 1. Thermo-physical properties of the PCM (RT100) [25] and Paraffin-Graphite composite

	Pure Paraffin	**Paraffin-Graphite composite (φ=15%)**
Melting temperature *[K]*	363-385 (typically 373)	363-385 (typically 373)
Latent heat capacity *[kJ/Kg]*	124	87.0
Thermal conductivity *[W/mK]* (solid-liquid)	0.2-0.2	15.0-15.0
Specific heat *[kJ/kg/K]* (solid-liquid)	1.8-2.4	1.48-1.82
Density *[kg/m^3]* (solid-liquid)	940-770	1136-992